MODIFIED SEQUENCE DOMAIN IMPEDANCE MODELLING OF THE MODULAR MULTILEVEL CONVERTER

Haoxiang Zong[1], Jing Lyu[1], Chen Zhang[2], Xu Cai[1], Marta Molinas[2], Fangquan Rao[1]*

[1] *Wind Power Research centre, Shanghai Jiao Tong University, Shanghai, China*
[2] *Department of Engineering Cybernetics, Norwegian University of Science and Technology, Trondheim, Norway*
* *xucai@sjtu.edu.cn*

Keywords: MODIFIED SEQUENCE DOMAIN, FREQUENCY COUPLING, HARMONIC STATE SPACE

Abstract

The accurate sequence impedance model of the modular multilevel converter (MMC) is essential for the precise stability analysis of various MMC-based interconnected systems. This paper presents a modified sequence impedance model for MMC considering off-diagonal coupling effects. Instead of simplifying the MMC as the single-phase model, the three-phase harmonic state-space model of the MMC is established based on harmonic state space theory. Then, the linear symmetric transformation is applied to transform the MMC's three-phase model into the modified sequence impedance model. The accuracy of the proposed model is validated by comparing with corresponding frequency scanning results in Matlab/Simulink. The research shows that there exist strong couplings between the positive and negative sequence of the MMC which cannot be ignored.

1 Introduction

With the fast growing of the large-scale wind farm, the demand for Modular Multilevel Converter (MMC) High Voltage Direct Current (HVDC) transmission schemes [1] has increased significantly in recent years. The MMC-HVDC has numerous advantages over the two-level Voltage Source Converter (VSC) HVDC, such as modularity, high efficiency, and reduced converter losses so on. However, the unique multi-frequency response characteristic of the MMC will result in multiple harmonic couplings in wide frequency range, which facilitate resonance and small-signal instability between the wind farm and the MMC-HVDC [2-5]. Therefore, it's essential to develop an accurate model which could depict multi-harmonic couplings between the positive and negative sequence in the MMC.

Recently, researchers have proposed several kinds of modelling methods to depict the ac-side impedance characteristics of the MMC, including the multi-harmonic linearization method [6], [7] and harmonic state-space method (HSS) [8]. The HSS method is getting more and more attention due to its advantages, like rigorousness, intuitive and capability of being extended to any number of harmonics. Therefore, in this paper, the HSS is selected to derive the modified sequence impedance model of the MMC. What's more, for simplicity, many researches [6-8] modelled MMC by simplifying the three-phase model into the single-phase model. However, in this paper, the derivation is based on the complete three-phase model of the MMC [9][10], which can include couplings between phases and is also able to be applied in asymmetric studies. Based on the concept of modified domain defined in [11], the couplings between the positive and negative sequence of the MMC can be taken into account in the modified sequence impedance model developed in this paper.

The rest of the paper is organized as below. In section 2, the periodic time-varying three-phase model of MMC is established including the main circuit and control parts. In section 3, the three-phase model of the MMC is linearized and transformed into modified sequence model based on HSS method. In section 4, the accuracy of the proposed modified sequence impedance model is validated in Matlab/Simulink. Based on this model, the off-diagonal couplings are analysed.

2 Three-Phase Model of the MMC

According to the conclusion in [11], the off-diagonal couplings can be neglected only when the system is mirror frequency decoupled. However, in the modular multilevel converter (MMC), there exist not only the asymmetric *d-q* control but also the internal multi-harmonic couplings. Therefore, even when the MMC operates under open-loop control, there will still exist strong off-diagonal couplings which will be shown in the following part. To better reflect these couplings, it's a good choice to use the modified domain sequence impedance [11]. The first step is to establish the three-phase model of the MMC. For simplicity, in this paper, the modified sequence impedance of the MMC under open loop control is established whose method could be applied under other control modes.

The topology of the MMC connected to a passive load is shown in Fig.1, with the open-loop control. Periodic time-varying model of the MMC has been studied well [12] and here the three-phase model is given in (1) ~ (4).

$$\frac{\mathrm{d}}{\mathrm{dt}}\boldsymbol{i}_{\mathrm{c}x} = -\frac{R}{L}\boldsymbol{i}_{\mathrm{c}x} - \frac{\boldsymbol{n}_{\mathrm{u}x}}{2L}\boldsymbol{v}_{\mathrm{cu}x} - \frac{\boldsymbol{n}_{\mathrm{l}x}}{2L}\boldsymbol{v}_{\mathrm{cl}x} + \frac{\boldsymbol{V}_{\mathrm{dc}}}{2L} \quad (1)$$

$$\frac{\mathrm{d}}{\mathrm{dt}}\boldsymbol{v}_{\mathrm{cu}x} = \frac{\boldsymbol{n}_{\mathrm{u}x}}{C_{\mathrm{arm}}}\left(\boldsymbol{i}_{\mathrm{c}x} + \frac{1}{2}\boldsymbol{i}_{\mathrm{g}x}\right) \quad (2)$$

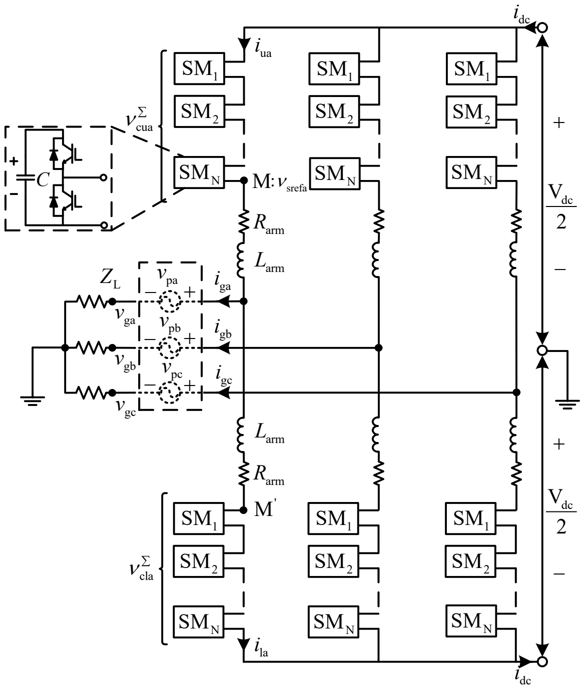

Fig. 1 The topology of the MMC

$$\frac{\mathrm{d}}{\mathrm{dt}}\boldsymbol{v}_{\mathrm{cl}x}=\frac{\boldsymbol{n}_{\mathrm{l}x}}{C_{\mathrm{arm}}}\left(\boldsymbol{i}_{\mathrm{c}x}-\frac{1}{2}\boldsymbol{i}_{\mathrm{g}x}\right) \tag{3}$$

$$\frac{\mathrm{d}}{\mathrm{dt}}\boldsymbol{i}_{\mathrm{g}x}=-\frac{\boldsymbol{n}_{\mathrm{u}x}}{L}\boldsymbol{v}_{\mathrm{cu}x}+\frac{\boldsymbol{n}_{\mathrm{l}x}}{L}\boldsymbol{v}_{\mathrm{cl}x}-\frac{R}{L}\boldsymbol{i}_{\mathrm{g}x}-\frac{2}{L}\boldsymbol{v}_{\mathrm{g}x} \tag{4}$$

Where the state variable $\boldsymbol{i}_{\mathrm{cx}}$, $\boldsymbol{v}_{\mathrm{cux}}$, $\boldsymbol{v}_{\mathrm{clx}}$, $\boldsymbol{i}_{\mathrm{gx}}$ are all 3×1 column vector, which represent the circulating current, upper arm voltage, lower arm voltage and the ac-side current in three-phase form. The subscript x represents the phase a, b, c. The meaning of the other symbols is labelled in Fig.1. The modulation signal of upper or lower arm is mainly composed of two parts, i.e., fundamental frequency control and circulating current control, which is given in (5)

$$\begin{cases}\boldsymbol{n}_{\mathrm{u}x}=\dfrac{1}{2}\boldsymbol{I}-\dfrac{\boldsymbol{v}_{\mathrm{gref}x}+\boldsymbol{v}_{\mathrm{cref}x}}{V_{\mathrm{dc}}}\\[2ex] \boldsymbol{n}_{\mathrm{l}x}=\dfrac{1}{2}\boldsymbol{I}+\dfrac{\boldsymbol{v}_{\mathrm{gref}x}-\boldsymbol{v}_{\mathrm{cref}x}}{V_{\mathrm{dc}}}\end{cases} \tag{5}$$

Under the open-loop control mode, the double frequency modulation signal $\boldsymbol{v}_{\mathrm{crefx}}$ can be set zero which means there exist only fundamental components in the modulation signal.

3 HSS-based Modified Sequence Impedance Model of the MMC

The principle of the HSS has been explained well in [8], whose essence is to transform the time-domain state space model into the frequency-domain multi-harmonic state space model according to the Fourier series and harmonic balance theory. The basic procedure could be divided into two steps, i.e., 1) the linearization of the state-space model in time-domain; 2) multi-harmonic expansion of the linearized state-space model.

3.1 Linearization of the three-phase model in time domain

Since the MMC operates under open loop control, the small-signal term of modulation signal will be zero. The linearized form of the equation (1) ~ (4) is given here.

$$\frac{\mathrm{d}}{\mathrm{dt}}\Delta\boldsymbol{i}_{\mathrm{c}x}=-\frac{R}{L}\Delta\boldsymbol{i}_{\mathrm{c}x}-\frac{\boldsymbol{n}_{\mathrm{u}x\mathrm{s}}}{2L}\Delta\boldsymbol{v}_{\mathrm{cu}x}-\frac{\boldsymbol{n}_{\mathrm{l}x\mathrm{s}}}{2L}\Delta\boldsymbol{v}_{\mathrm{cl}x} \tag{6}$$

$$\frac{\mathrm{d}}{\mathrm{dt}}\Delta\boldsymbol{v}_{\mathrm{cu}x}=\frac{\boldsymbol{n}_{\mathrm{u}x\mathrm{s}}}{C_{\mathrm{arm}}}\left(\Delta\boldsymbol{i}_{\mathrm{c}x}+\frac{1}{2}\Delta\boldsymbol{i}_{\mathrm{g}x}\right) \tag{7}$$

$$\frac{\mathrm{d}}{\mathrm{dt}}\Delta\boldsymbol{v}_{\mathrm{cl}x}=\frac{\boldsymbol{n}_{\mathrm{l}x\mathrm{s}}}{C_{\mathrm{arm}}}\left(\Delta\boldsymbol{i}_{\mathrm{c}x}-\frac{1}{2}\Delta\boldsymbol{i}_{\mathrm{g}x}\right) \tag{8}$$

$$\frac{\mathrm{d}}{\mathrm{dt}}\Delta\boldsymbol{i}_{\mathrm{g}x}=\frac{\boldsymbol{n}_{\mathrm{l}x\mathrm{s}}}{L}\Delta\boldsymbol{v}_{\mathrm{cl}x}-\frac{\boldsymbol{n}_{\mathrm{u}x\mathrm{s}}}{L}\Delta\boldsymbol{v}_{\mathrm{cu}x}-\frac{R+Z_{\mathrm{L}}}{L}\Delta\boldsymbol{i}_{\mathrm{g}x} \tag{9}$$

The expression of $\boldsymbol{A}_{\mathrm{s}}$ is given in (10).

$$\boldsymbol{A}_s=\begin{bmatrix}-\dfrac{R}{L}\cdot\boldsymbol{I}_{3\times3} & -\dfrac{\boldsymbol{n}_{\mathrm{u}x\mathrm{s}}}{2L} & -\dfrac{\boldsymbol{n}_{\mathrm{l}x\mathrm{s}}}{2L} & \boldsymbol{0}_{3\times3}\\[2ex] \dfrac{\boldsymbol{n}_{\mathrm{u}x\mathrm{s}}}{C_{\mathrm{arm}}} & \boldsymbol{0}_{3\times3} & \boldsymbol{0}_{3\times3} & \dfrac{\boldsymbol{n}_{\mathrm{u}x\mathrm{s}}}{2\cdot C_{\mathrm{arm}}}\\[2ex] \dfrac{\boldsymbol{n}_{lx\mathrm{s}}}{C_{\mathrm{arm}}} & \boldsymbol{0}_{3\times3} & \boldsymbol{0}_{3\times3} & \dfrac{\boldsymbol{n}_{lx\mathrm{s}}}{2\cdot C_{\mathrm{arm}}}\\[2ex] \boldsymbol{0}_{3\times3} & -\dfrac{\boldsymbol{n}_{\mathrm{u}x\mathrm{s}}}{L} & \dfrac{\boldsymbol{n}_{\mathrm{l}x\mathrm{s}}}{L} & -\dfrac{R+Z_{\mathrm{L}}}{L}\cdot\boldsymbol{I}_{3\times3}\end{bmatrix}_{12\times12} \tag{10}$$

The $\boldsymbol{n}_{\mathrm{uxs}}$ and $\boldsymbol{n}_{\mathrm{lxs}}$ represent the modulation ratio of the upper and lower arm in *abc* form respectively as shown in (11).

$$\boldsymbol{n}_{\mathrm{u}x\mathrm{s}}=\begin{bmatrix}n_{\mathrm{uas}} & 0 & 0\\ 0 & n_{\mathrm{ubs}} & 0\\ 0 & 0 & n_{\mathrm{ucs}}\end{bmatrix},\ \boldsymbol{n}_{lx\mathrm{s}}=\begin{bmatrix}n_{\mathrm{las}} & 0 & 0\\ 0 & n_{\mathrm{lbs}} & 0\\ 0 & 0 & n_{\mathrm{lcs}}\end{bmatrix} \tag{11}$$

Here, the steady value of the three-phase modulation signal in frequency domain is given in table 1.

Table 1 Modulation ratio in the frequency domain

	s	Value		
Phase		*a*	*b*	*c*
Upper Arm	0	0.5	0.5	0.5
	+1	$-\frac{1}{4}m$	$-\frac{1}{4}me^{-j\frac{2\pi}{3}}$	$-\frac{1}{4}me^{j\frac{2\pi}{3}}$
	-1	$-\frac{1}{4}m$	$-\frac{1}{4}me^{j\frac{2\pi}{3}}$	$-\frac{1}{4}me^{-j\frac{2\pi}{3}}$
Lower Arm	0	0.5	0.5	0.5
	+1	$-\frac{1}{4}me^{-j\pi}$	$-\frac{1}{4}me^{j\frac{1}{3}\pi}$	$-\frac{1}{4}me^{-j\frac{1}{3}\pi}$
	-1	$-\frac{1}{4}me^{j\pi}$	$-\frac{1}{4}me^{-j\frac{1}{3}\pi}$	$-\frac{1}{4}me^{j\frac{1}{3}\pi}$

Since the MMC operates under the open loop control, the steady harmonic value of the modulation signal higher than the first order will be zero.

3.2 HSS model of the MMC in frequency domain

Since the linearized state-space model of the MMC has been gotten in (6) ~ (9), the next step is to implement the harmonic expansion on the state-space model. The procedure of transforming the time-domain state-space model into frequency-domain harmonic state-space model has been explained well in [8] and here the results are listed. The Toeplitz matrix $\boldsymbol{A}$ at each harmonic is shown in (12).

$$\boldsymbol{A}=\begin{pmatrix} A_0 & A_{-1} & \cdots & A_{-h} & & & \\ A_1 & \ddots & \ddots & \ddots & \ddots & & \\ \vdots & \ddots & A_0 & A_{-1} & \ddots & \ddots & \\ A_h & \ddots & A_1 & A_0 & A_{-1} & \ddots & A_{-h} \\ & \ddots & \ddots & A_1 & A_0 & \ddots & \vdots \\ & & \ddots & \ddots & \ddots & \ddots & A_{-1} \\ & & & A_h & \cdots & A_1 & A_0 \end{pmatrix} \tag{12}$$

According to the conclusion in [8], the accuracy can be guaranteed when the harmonic order h is set 4, i.e., s=0, ±1, ±2, ±3, ±4. Each harmonic value of each state variable can be calculated via the equation (13).

$$\boldsymbol{X}_p=-\left(\boldsymbol{A}-\boldsymbol{N}_p\right)^{-1}\cdot\boldsymbol{U}_p \tag{13}$$

Since the modulation signal is composed of only fundamental components, the matrix $\boldsymbol{A}_s$ higher than triple frequency can be set as zero matrix.

$$\boldsymbol{A}_{2\ldots h}=\boldsymbol{A}_{-2\ldots -h}=\boldsymbol{O}^{12\times12} \tag{14}$$

The state variables of the HSS model (h=4) include:

$$\mathbf{X}_p=\begin{bmatrix} \boldsymbol{X}_{(\omega_p-4\omega_1)} \\ \vdots \\ \boldsymbol{X}_{(\omega_p-\omega_1)} \\ \boldsymbol{X}_{(\omega_p)} \\ \boldsymbol{X}_{(\omega_p+\omega_1)} \\ \vdots \\ \boldsymbol{X}_{(\omega_p+4\omega_1)} \end{bmatrix},\boldsymbol{X}_{(\omega_p\pm h\omega_1)}=\begin{bmatrix} \boldsymbol{I}_{cx(\omega_p\pm h\omega_1)} \\ \boldsymbol{V}^{\Sigma}_{cux(\omega_p\pm h\omega_1)} \\ \boldsymbol{V}^{\Sigma}_{clx(\omega_p\pm h\omega_1)} \\ \boldsymbol{I}_{gx(\omega_p\pm h\omega_1)} \end{bmatrix} \tag{15}$$

The component of the $\boldsymbol{N}_\mathrm{p}$ in (13) is given in (16).

$$\boldsymbol{N}_p=\begin{bmatrix} j(\omega_p-4\omega_1)\boldsymbol{I} & & & & \\ & \ddots & & & \\ & & j\omega_p\boldsymbol{I} & & \\ & & & \ddots & \\ & & & & j(\omega_p+4\omega_1)\boldsymbol{I} \end{bmatrix} \tag{16}$$

Where the $\boldsymbol{I}$ represents the 12×12 unit matrix. The external disturbance three-phase voltage shown in Fig.1 is used as the input variable of the HSS model.

$$\boldsymbol{U}_p=\begin{bmatrix} \boldsymbol{U}_{(\omega_p-4\omega_1)} \\ \vdots \\ \boldsymbol{U}_{(\omega_p-\omega_1)} \\ \boldsymbol{U}_{(\omega_p)} \\ \boldsymbol{U}_{(\omega_p+\omega_1)} \\ \vdots \\ \boldsymbol{U}_{(\omega_p+4\omega_1)} \end{bmatrix},\boldsymbol{U}_{(\omega_p)}=\begin{bmatrix} \mathbf{0}_{3\times1} \\ \mathbf{0}_{3\times1} \\ \mathbf{0}_{3\times1} \\ V_p \\ V_p e^{-j\frac{2\pi}{3}} \\ V_p e^{j\frac{2\pi}{3}} \end{bmatrix},\boldsymbol{U}_{(\omega_p\pm h\omega_1)}=\boldsymbol{O}^{12\times1} \tag{17}$$

Here, the positive sequence voltage disturbance is selected as an injection example.

3.3 Modified sequence impedance model of the MMC

According to the above section, each harmonic value of each state variable has been calculated. In this part, the linear symmetric transform is applied in the calculated results in *abc* frame to acquire the sequence components in frequency domain.

$$\boldsymbol{E}=\begin{bmatrix} \boldsymbol{e}^{2\times3} & & & & \\ & \boldsymbol{e}^{2\times3} & & & \\ & & \boldsymbol{e}^{2\times3} & & \\ & & & \boldsymbol{e}^{2\times3} & \\ & & & & \boldsymbol{e}^{2\times3} \end{bmatrix}_{8\times12} \tag{18}$$

$$\boldsymbol{e}=\frac{1}{3}\begin{bmatrix} 1 & e^{j\frac{2\pi}{3}} & e^{-j\frac{2\pi}{3}} \\ 1 & e^{-j\frac{2\pi}{3}} & e^{j\frac{2\pi}{3}} \end{bmatrix}_{2\times3} \tag{19}$$

Therefore, the sequence components of the ac-side voltage and current can be gotten.

$$\boldsymbol{I}_{gpn}=\boldsymbol{E}\begin{bmatrix} \boldsymbol{I}_{gx(\omega_p-4\omega_1)} \\ \vdots \\ \boldsymbol{I}_{gx(\omega_p-\omega_1)} \\ \boldsymbol{I}_{gx(\omega_p)} \\ \boldsymbol{I}_{gx(\omega_p+\omega_1)} \\ \vdots \\ \boldsymbol{I}_{gx(\omega_p+4\omega_1)} \end{bmatrix},\boldsymbol{V}_{gpn}=\boldsymbol{E}\left(\begin{bmatrix} \boldsymbol{I}_{gx(\omega_p-4\omega_1)} \\ \vdots \\ \boldsymbol{I}_{gx(\omega_p-\omega_1)} \\ \boldsymbol{I}_{gx(\omega_p)} \\ \boldsymbol{I}_{gx(\omega_p+\omega_1)} \\ \vdots \\ \boldsymbol{I}_{gx(\omega_p+4\omega_1)} \end{bmatrix}Z_L+\begin{bmatrix} \mathbf{0}_{3\times1} \\ \vdots \\ \mathbf{0}_{3\times1} \\ \boldsymbol{V}_{px} \\ \mathbf{0}_{3\times1} \\ \vdots \\ \mathbf{0}_{3\times1} \end{bmatrix}\right) \tag{20}$$

As stated in [11], the 2×2 modified sequence matrix needs two independent injections, for example, positive sequence injection and negative sequence injection. With these two independent sets of the disturbed ac-side voltage and current, the modified sequence impedance can be derived as.

$$\begin{bmatrix} Z_{pp} & Z_{pn} \\ Z_{np} & Z_{nn} \end{bmatrix} = \begin{bmatrix} V_{p1} & V_{p2} \\ V_{n1} & V_{n2} \end{bmatrix} \begin{bmatrix} I_{p1} & I_{p2} \\ I_{n1} & I_{n2} \end{bmatrix}^{-1} \tag{21}$$

For the positive sequence voltage disturbance injection ($\boldsymbol{V}_{px}$=[V_p $V_p e^{-j2\pi/3}$ $V_p e^{j2\pi/3}$]^T), the corresponding ac-side voltage and current in sequence form is extracted as.

$$\begin{aligned} V_{p1} &= V_{gpn}^{\mathrm{P}}(\omega_p), \quad I_{p1} = I_{gpn}^{\mathrm{P}}(\omega_p), \\ V_{n1} &= V_{gpn}^{\mathrm{N}}(\omega_p - 2\omega_1), \quad I_{n1} = I_{gpn}^{\mathrm{N}}(\omega_p - 2\omega_1) \end{aligned} \tag{22}$$

For the negative sequence voltage disturbance injection ($\boldsymbol{V}_{px}$=[V_n $V_n e^{j2\pi/3}$ $V_n e^{-j2\pi/3}$]^T), the corresponding ac-side voltage and current in sequence form is extracted as.

$$\begin{aligned} V_{n2} &= V_{gpn}^{\mathrm{N}}(\omega_n), \quad I_{n2} = I_{gpn}^{\mathrm{N}}(\omega_n) \\ V_{p2} &= V_{gpn}^{\mathrm{P}}(\omega_n + 2\omega_1), \quad I_{p2} = I_{gpn}^{\mathrm{P}}(\omega_n + 2\omega_1) \end{aligned} \tag{23}$$

4 Results

In this part, the correctness of the derived modified sequence impedance model of the MMC is verified by frequency scanning. The main MMC's parameters are listed in Table 2.

Table 2 Main Parameters of the MMC

Parameters	Value
Arm resistance	1 Ω
Arm inductance	360 mH
Sub-module capacitance	140 µF
Number of arm sub-modules	20
Dc-link Voltage	320 kV
Grid frequency	50 Hz
Resistance of passive load	551.2 Ω

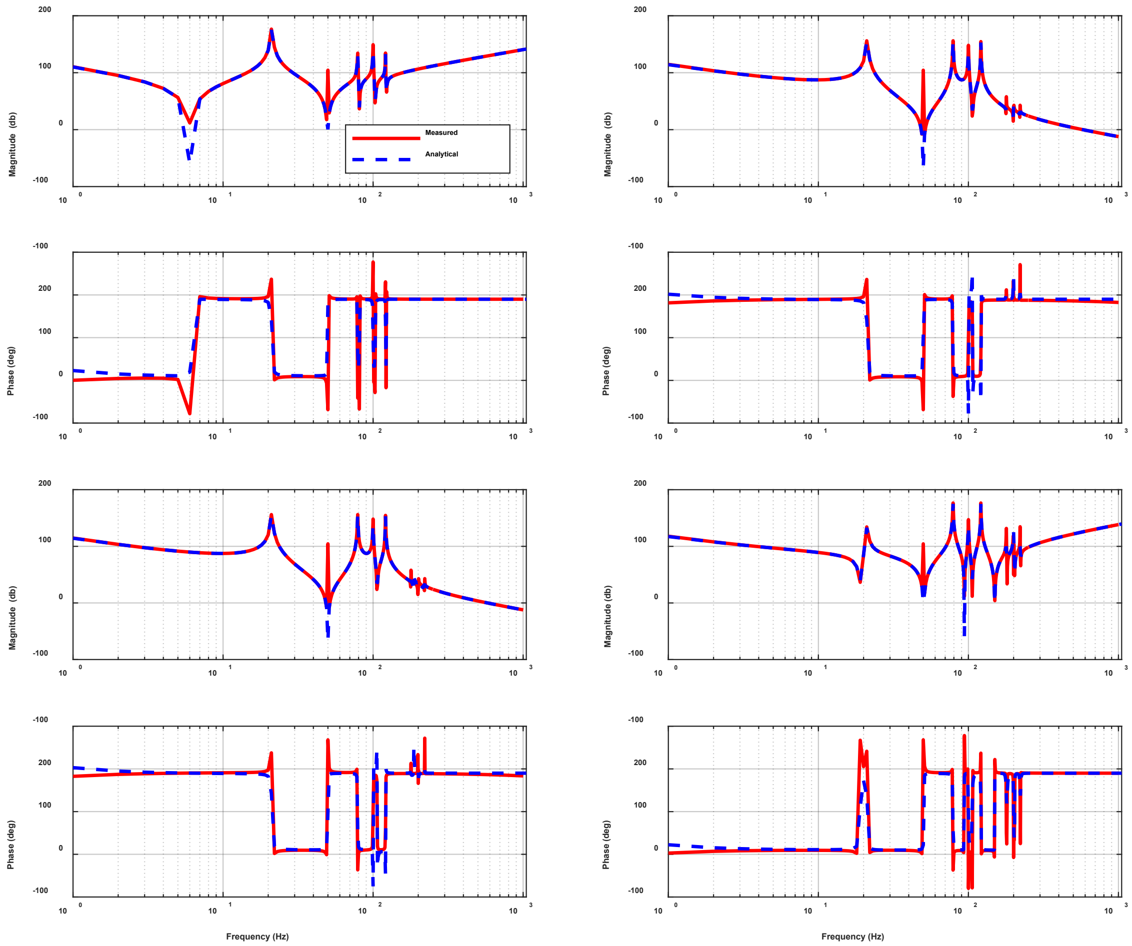

Fig. 2 Impedance verification of the derived MMC model under open-loop control

As shown in Fig. 2, the analytical impedance curves are consistent with frequency scanning impedance curves in diagonal and off-diagonal components, including magnitude and phase curves. The correctness of the proposed modified sequence impedance model of the MMC is verified under open-loop control. It can be observed that the off-diagonal component is relatively high especially in low frequency range, whose peak value is nearly the same as that of the Z_{pp} around 20Hz. However, in high-frequency range, the effect of off-diagonal couplings could be neglected whose amplitude is almost zero. What's more, under open loop control, the off-diagonal components are almost equal to each other.

5 Conclusion

In this paper, the modified sequence impedance model of the MMC under open loop control is developed. This method could be extended to other kinds of control modes similarly. The effects of the off-diagonal couplings are analysed briefly. In the future work, various control modes will also be modelled and analysed, like the ac-voltage control, the power control, the circulating current suppress control and the direct-current voltage control. It can be concluded that there exists inherent coupling between the positive and negative sequence impedance. The effects of such couplings on the stability analysis will also be presented in the future work.

6 Acknowledgements

This work was supported by the National Natural Science Foundation of China under Grant 51837007. The authors would like to thank team members at SJTU, and co-workers from NTNU for their valuable advices.

7 References

[1] Debnath, S., Qin, J., Bahrani, B., et al.: 'Operation, Control, and Applications of the Modular Multilevel Converter: A Review', IEEE Transactions on Power Electronics., 2015, 30, (1), pp. 37-53

[2] Lyu, J., Cai, X., Molinas, M.: 'Frequency domain stability analysis of MMC-based HVdc for wind farm integration', IEEE Journal of Emerging and Selected Topics in Power Electronics., 2016, 4, (1), pp. 141-151

[3] Lyu, J., Cai, X., Amin, M., Molinas, M.: 'Subsynchronous oscillation mechanism and its suppression in MMC-Based HVDC connected wind farms', IET Generation, Transmission & Distribution., 2018, 12, (4), pp. 1021-1029

[4] Zong, H., Lyu, J., Cai, X., M., Molinas, et al.: 'Analysis of Bifurcation Behaviors in MMC Connected to a Weak Grid, ' IECON 2018 - 44th Annual Conference of the IEEE Industrial Electronics Society, Washington, DC, 2018, pp. 1687-1692

[5] Lyu, J., Cai, X., Molinas, M.: 'Optimal design of controller parameters for improving the stability of MMC-HVDC for wind farm integration', IEEE Journal of Emerging and Selected Topics in Power Electronics, 2018, 6, (1), pp. 40-53

[6] Sun, J. and Liu, H.: 'Sequence Impedance Modeling of Modular Multilevel Converters', IEEE Journal of Emerging and Selected Topics in Power Electronics., 2017, 5, (4), pp. 1427-1443

[7] Sun, J. and Liu, H.: 'Impedance modeling and analysis of modular multilevel converters', 2016 IEEE 17th Workshop on Control and Modeling for Power Electronics (COMPEL), Trondheim, 2016, pp. 1-9

[8] Lyu, J., Zhang, X., Cai, X., and Molinas, M.: 'Harmonic state-space based small-signal impedance modeling of modular multilevel converter with consideration of internal harmonic dynamics', IEEE Transactions on Power Electronics., 2019, 34, (3), pp. 2134-2148

[9] Chen, Q., Lyu, J., Li, R., et al.: 'Impedance modeling of modular multilevel converter based on harmonic state space, ' 2016 IEEE 17th Workshop on Control and Modeling for Power Electronics (COMPEL), Trondheim, 2016, pp. 1-5

[10] Lyu, J., Cai, X., Zhang, X., et al.: 'Harmonic state space modeling and analysis of modular multilevel converter', IEEE PEAC, Shenzhen, China, Nov. 2018, pp. 1-6

[11] Rygg, A., Molinas, M., Zhang, C. and Cai, X.: 'A Modified Sequence-Domain Impedance Definition and Its Equivalence to the dq-Domain Impedance Definition for the Stability Analysis of AC Power Electronic Systems', IEEE Journal of Emerging and Selected Topics in Power Electronics., 2016, 4, (4), pp. 1383-1396

[12] Gilbert, Bergna., Suul, J. A., and D'Arco, S.: 'State-space modelling of modular multilevel converters for constant variables in steady-state', 2016 IEEE 17th Workshop on Control and Modeling for Power Electronics (COMPEL), Trondheim, 2016, pp. 1-9